DOI: 10.1002/adma.200501464

Recent Advances in Chemical Synthesis, Self-Assembly, and Applications of FePt Nanoparticles**

By *Shouheng Sun**

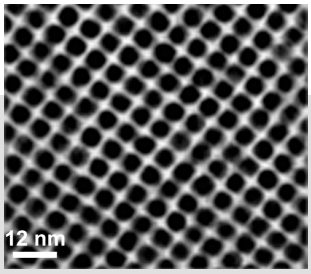

This paper reviews recent advances in chemical synthesis, self-assembly, and potential applications of monodisperse binary FePt nanoparticles. After a brief introduction to nanomagnetism and conventional processes of fabricating FePt nanoparticles, the paper focuses on recent developments in solution-phase syntheses of monodisperse FePt nanoparticles and their self-assembly into nanoparticle superlattices. The paper further outlines the surface, structural, and magnetic properties of the FePt nanoparticles and gives examples of three potential applications in data storage, permanent magnetic nanocomposites, and biomedicine.

1. Introduction

Magnetic nanoparticles with sizes ranging from 2 to 20 nm in diameter represent an important class of artificial nanostructured materials. Their magnetic properties change drastically with their size, as the relaxation of the magnetization orientation of each particle is determined by $\tau = \tau_0 e^{KV/2kT}$, in which τ is the relaxation time at one orientation, K is the particle's anisotropy constant, V is the particle volume, k is Boltzmann's constant, and T is temperature.[1,2] The term KV measures the energy barrier between two orientations. As the size of the particle decreases to a level where KV becomes comparable to the thermal energy kT, its magnetization starts to fluctuate from one direction to another. As a result, at this T the overall magnetic moment of this particle is randomized to zero, and the particle is said to be superparamagnetic.

The magnetic behavior of a group of magnetic nanoparticles can be better described by a hysteresis loop that measures the change of magnetic moment (M) over the strength of an applied magnetic field (H). As shown in Figure 1A, in the absence of an external field (center point), the magnetization of each particle points in different directions and the overall magnetic moment is zero. When an external magnetic field is applied, magnetic interaction between the particles and the field aligns the magnetization of the particles along the field direction. When the field is strong enough, all particles are aligned in the field direction and the particles are said to be

[*] Dr. S. Sun
Department of Chemistry
Brown University
Providence, RI 02912 (USA)
E-mail: ssun@brown.edu

[**] The author thanks Drs. C. B. Murray, G. A. Held, H. F. Hamann, D. Weller, A. Moser, L. Folks, S. Raoux, E. E. Fullerton, T. Thomason, M. F. Toney, J. E. E. Baglin, P. M. Rice, B. D. Terris and his postdoctoral associates, Drs. H. Zeng, D. B. Robinson, H. Yu, and M. Chen at IBM research for their important contributions to FePt nanoparticle research. The author also thanks Prof. P. Liu of the University of Texas, Arlington, Prof. S. Wang of Stanford University, and Prof Z. L. Wang of the Georgia Institute of Technology for their collaboration in nanocomposite and biomagnetic projects. The research has been supported by DARPA/ARO, DARPA/ONR, ONR/MURI, Hitachi Maxell, Ltd., and Brown University.

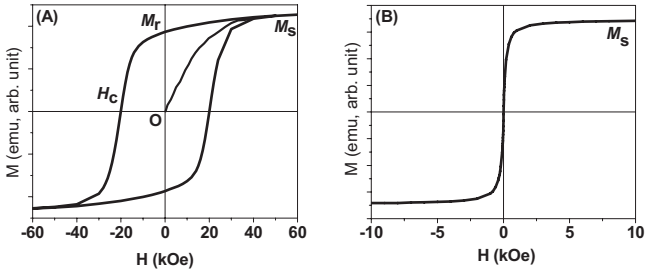

Figure 1. Schematic illustration of the hysteresis loops of a group of magnetic nanoparticles that are A) ferromagnetic and B) superparamagnetic. M_S: saturation magnetic moment; M_r: remnant magnetic moment.

saturated; the corresponding moment is called the saturation moment (M_s). Reducing the strength of the field leads to randomization of the magnetization and a smaller magnetic moment. When the external field drops to zero, the ferromagnetic particles retain a considerable degree of magnetization with a net measurable moment: the remnant magnetic moment (M_r). (This serves as a basis for magnetic memory devices). To demagnetize the particles, the external field must be reversed and increased to a value where the total moment is zero. This value is called the coercivity (H_c). If the particles are superparamagnetic, the magnetization of each particle undergoes thermal fluctuation. As long as the field is removed, the overall moment is randomized to zero, leaving no remnant magnetic moment (Fig. 1B). This superparamagnetism of magnetic nanoparticles becomes the fundamental density limit for magnetic memory devices.[3,4] Interestingly, these superparamagnetic nanoparticles are very useful for biomedical applications, as they are not subject to strong magnetic interactions in a dispersion and are stable in physiological conditions.[5–7]

FePt nanoparticles containing a near-equal atomic percentage of Fe and Pt are an important class of magnetic nanomaterials. They are known to have a chemically disordered face-centered cubic (fcc) structure or a chemically ordered face-centered tetragonal (fct) structure,[8] as shown in Figure 2. The fcc-structured FePt has a small coercivity and is magnetically soft. The fully ordered fct-structured FePt can be viewed as alternating atomic layers of Fe and Pt stacked along the [001] direction (the *c*-axis in Fig. 2B). The anisotropy constant *K*, which measures the ease of magnetization reversal along the easy axis, can reach as high as 10^7 J m^{-3},[3] a value that is one of the largest among all known hard magnetic materials. This large *K* is caused by Fe and Pt interactions originating from spin-orbit coupling and the hybridization between Fe 3d and Pt 5d states.[9–12] These Fe–Pt interactions further render the FePt nanoparticles chemically much more stable than the common high-moment nanoparticles of Co and Fe, as well as the large coercive materials $CoSm_5$ and $Nd_2Fe_{14}B$, making them especially useful for practical applications in solid-state devices and biomedicine.

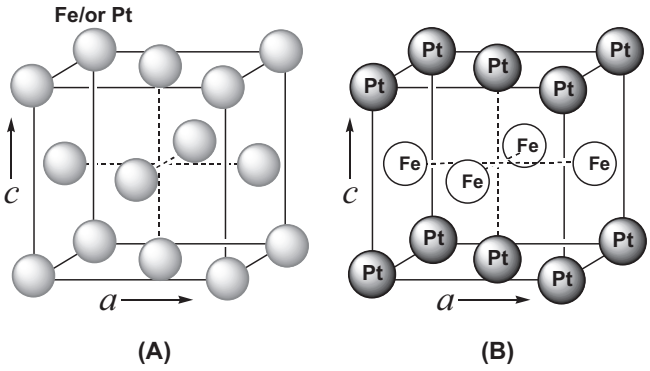

Figure 2. Schematic illustration of the unit cell of A) chemically disordered fcc and B) chemically ordered fct FePt.

FePt nanoparticles are commonly fabricated using vacuum-deposition techniques.[13–15] As deposited, the FePt has a chemically disordered fcc structure and is magnetically soft. Thermal annealing is needed to transform the fcc structure into the chemically ordered fct structure. However, the annealing also results in particle aggregation, leading to wide size distributions. To control the size and narrow the size distribution, FePt nanoparticles prepared from vacuum-deposition methods are often buried in a variety of insulator matrices, such as SiO_2,[16] Al_2O_3,[17] B_2O_3,[18] or Si_3N_4.[19] Alternatively, FePt particles can be made by gas-phase evaporation.[20] Although the average size of these particles can be better controlled in the improved syntheses, it is still difficult to disperse them in various liquid media and to use them to form regular arrays. In contrast with all the physical deposition processes, solution-phase synthesis offers a unique way for producing monodisperse nanoparticles,[21–25] and has been found to be particularly effective in synthesizing monodisperse FePt nanoparticles and nanoparticle superlattices. This paper briefly reviews the recent progress in chemical syntheses and self-assembly of monodisperse FePt nanoparticles as well as their potential applications in data storage, permanent magnetic nanocomposites, and biomedicine.

Shouheng Sun is an Associate Professor of Chemistry and Engineering at Brown University. He received his B.Sc. from Sichuan University (China, 1984), his M.Sc. from Nanjing University (China, 1987), and his Ph.D. from Brown University (1996), all in chemistry. He was a Lecturer in the Department of Chemistry and Coordination Chemistry Institute of Nanjing University from 1987–1992. He joined IBM's Thomas J. Watson Research Center at Yorktown Heights, New York, first as a postdoctoral associate in 1996 and then as a research staff member from 1998–2004. He moved to Brown's Chemistry Department in January of 2005. His research interests include nanomaterials synthesis, self-assembly and applications in data storage, nanocomposites, catalysis, and biomedicine.

ADVANCED MATERIALS

2. Chemical Synthesis of FePt Nanoparticles

2.1. Synthesis of FePt Nanoparticles via Thermal Decomposition of $Fe(CO)_5$ and Reduction of $Pt(acac)_2$

Thermal decomposition of iron pentacarbonyl, $Fe(CO)_5$, and reduction of platinum acetylacetonate, $Pt(acac)_2$, in the presence of 1,2-alkanediol is a common synthesis route to monodisperse FePt nanoparticles.[26,27] The synthetic chemistry is illustrated in Figure 3. $Fe(CO)_5$ is thermally unstable and subject to decomposition at high temperature to carbon monoxide and Fe. This decomposition reaction has been utilized to prepare various Fe-based nanoparticles.[25] $Pt(acac)_2$ is readily reduced by a mild reducing agent, 1,2-alkanediol, to Pt. A small group of Fe and Pt atoms combine to form [Fe–Pt] clusters that act as nuclei. The growth proceeds as more Fe–Pt species deposit around the nuclei, forming FePt nanoparticles. Oleic acid and oleylamine (or similar long chain carboxylic acids and primary amines) are used for FePt nanoparticle surface passivation and particle stabilization. In a typical synthesis,[26] $Pt(acac)_2$ (197 mg, 0.5 mmol), 1,2-hexadecanediol (390 mg, 1.5 mmol), and dioctyl ether (20 mL) are first loaded in a reaction flask and stirred using a magnetic stirring bar. The mixture is heated to 100 °C under a gentle flow of N_2 to remove oxygen and moisture. Oleic acid (0.16 mL, 0.5 mmol) and oleylamine (0.17 mL, 0.5 mmol) are added to the mixture, and, after 10 min, the N_2 outlet is closed and the reaction system protected under a blanket of N_2. $Fe(CO)_5$ (0.13 mL, 1 mmol) is then introduced into the mixture, which is then further heated to reflux (297 °C). The refluxing is continued for 30 min. The heat source is then removed, and the reaction mixture allowed to cool to room temperature. The inert gas protected system is opened to ambient environment at this point. The black product is precipitated by adding ethanol (40 mL) and separated by centrifugation. The yellow-brown supernatant is discarded. The black precipitate is dispersed in hexane (25 mL) in the presence of oleic acid (0.05 mL) and oleylamine (0.05 mL) and precipitated out by adding ethanol (20 mL) and centrifuging. The product is dispersed in hexane (20 mL), centrifuged to remove any insoluble precipitate (almost no precipitation was found at this stage), and precipitated out by adding ethanol (15 mL) and centrifuging. The FePt nanoparticles can be dispersed in any alkane, arene, or chlorinated solvent.

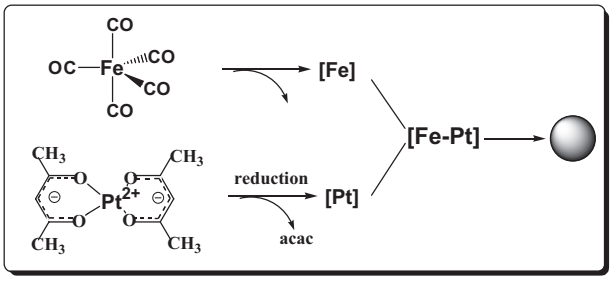

Figure 3. Schematic illustration of FePt nanoparticle formation from the decomposition of $Fe(CO)_5$ and reduction of $Pt(acac)_2$.

In the reaction condition described above, the composition of the FePt particles is controlled by the $Fe(CO)_5/Pt(acac)_2$ ratio.[27] Figure 4 shows the composition relation to the amount of $Fe(CO)_5$ added in the presence of a fixed amount of $Pt(acac)_2$ (0.5 mmol). It can be seen that not all of the $Fe(CO)_5$ contributes to the FePt-alloy formation. $Fe(CO)_5$ has a low boiling point (103 °C). At a reaction temperature of 297 °C, $Fe(CO)_5$ is actually in the vapor phase. The formation of this vapor phase likely results in the slow decomposition of $Fe(CO)_5$ at a rate that matches the reduction rate of $Pt(acac)_2$. The FePt nanoparticles are formed in a shorter period of time. Therefore, the consumption of $Fe(CO)_5$ cannot be completed within the synthesis time period. As a result, 0.5 mmol of $Fe(CO)_5$ and 0.5 mmol of $Pt(acac)_2$ yield $Fe_{38}Pt_{62}$, while 1.1 mmol of $Fe(CO)_5$ and 0.5 mmol of $Pt(acac)_2$ produce $Fe_{56}Pt_{44}$.

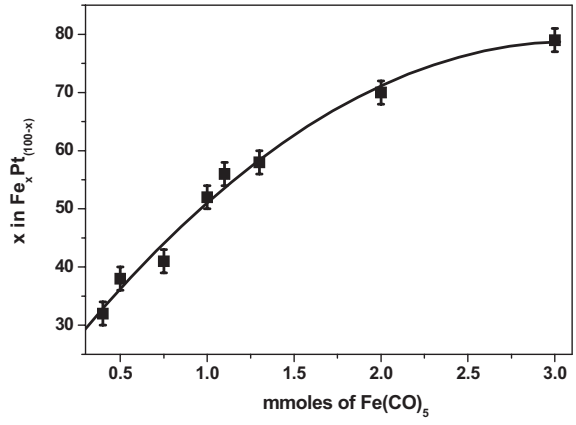

Figure 4. Compositional relation between $Fe(CO)_5$ and x in $Fe_xPt_{(100-x)}$ based on the reaction of $Fe(CO)_5$ with 0.5 mmol of $Pt(acac)_2$. Reprinted with permission from [27]. Copyright 2001 IEEE Magnetic Society.

Fine-tuning of the sizes of the FePt nanoparticles between 2 and 5 nm is achieved by controlling the surfactant to metal ratio.[28] Alternatively, to make larger FePt particles, a seed-mediated growth method is used.[26] This is performed by first making monodisperse 3–4 nm seed FePt particles, and then adding more Fe and Pt precursors to enlarge the existing FePt particle seeds to obtain the desired sizes.

Better control of the size of the FePt nanoparticles is obtained via a one-step simultaneous thermal decomposition of $Fe(CO)_5$ and reduction of $Pt(acac)_2$ in the absence of 1,2-alkanediol.[29] It is believed that 1,2-alkanediol can lead to the facile reduction of $Pt(acac)_2$ to Pt, resulting in fast nucleation of FePt and consumption of metal precursors, and, as a result, smaller particles. Exclusion of additional reducing agent in the reaction mixture slows down the nucleation rate, allowing more metal precursors to deposit around the nuclei, leading to a larger particle size. The particle formation mechanism is shown in Figure 5A. The Pt-rich nuclei (a) are formed from

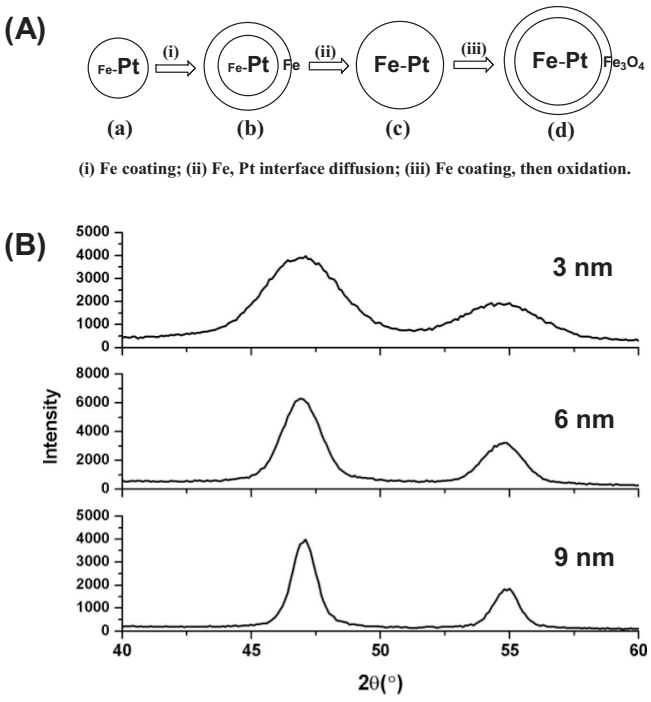

Figure 5. A) Schematic illustration of FePt nanoparticle formation mechanism and B) X-ray diffraction patterns of the as-synthesized FePt nanoparticles of different sizes. Reprinted with permission from [29]. Copyright 2004 American Chemical Society.

the simultaneous reduction of $Pt(acac)_2$ and partial decomposition of $Fe(CO)_5$ at temperatures less than 200 °C. More Fe atoms will then coat the existing Pt-rich nuclei, forming larger clusters (b) at a higher temperature. Heating the clusters (b) to reflux at 300 °C leads to atomic diffusion and formation of fcc-structured FePt nanoparticles (c). In the presence of excess of $Fe(CO)_5$, the extra Fe will continue to coat over (c), leading to core/shell structured FePt/Fe that is further oxidized to $FePt/Fe_3O_4$ (d). The size of the particles is tuned by controlling the molar ratio of the stabilizers to $Pt(acac)_2$ and heating conditions. A ratio of at least 8:1 is necessary to make FePt nanoparticles larger than 6 nm. At a fixed ratio of 8:1, both heating rate and interim heating temperature are important in tuning the sizes of the FePt particles. Applying a heating rate of ~15 °C min^{-1} and an interim heating temperature of 240 °C leads to 6 nm diameter FePt, while a slower rate of ~5 °C min^{-1} and a lower heating temperature of 225 °C yields 9 nm diameter FePt. Figures 5B shows the X-ray diffraction (XRD) patterns of the FePt nanoparticles with sizes of 3, 6, and 9 nm, in which the narrowed peak width reflects the large size of the crystallites.

In this one-step synthesis, the shape of the particles is controlled by sequential addition of the surfactants. By first mixing oleic acid, $Fe(CO)_5$, and $Pt(acac)_2$, and heating the mixture at 130 °C for about 5 min before oleylamine is added, highly faceted FePt nanoparticles are obtained (Fig. 6A).[29]

FePt nanoparticles have also been produced by sequential reduction of $Pt(acac)_2$ and thermal decomposition of

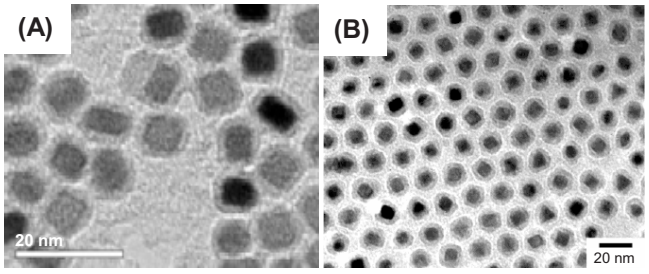

Figure 6. Transmission electron microscopy images of A) 7 nm cube-like FePt (reprinted with permission from [29]; copyright 2004 American Chemical Society) and B) Pt/Fe_2O_3 core/shell nanoparticles with 10 nm cores and 3.5 nm shells (reprinted with permission from [30]; copyright 2003 American Chemical Society).

$Fe(CO)_5$, followed by oxidation and reductive annealing.[30,31] In this synthesis, Pt nanoparticles are first made via the polyol reduction of $Pt(acac)_2$ in dioctyl ether. A layer of Fe_2O_3 is then coated over the Pt nanoparticles via thermal decomposition of $Fe(CO)_5$ and oxidation. The dimensions of the Pt core and the Fe_2O_3 shell are controlled by the amount of Pt or Fe precursors, respectively, used in the reaction. To make FePt nanoparticles, the $FePt/Fe_2O_3$ is further annealed under a gas mixture of H_2 (5 %) and Ar at 550 °C or above for 9 h. This high-temperature reductive annealing has two purposes: to reduce Fe_2O_3 to Fe and to make Fe and Pt diffuse into FePt alloy particles. Figure 6B shows Pt/Fe_2O_3 core/shell particles with 10 nm diameter Pt cores and 3.5 nm thick Fe_2O_3 shells. After reductive annealing, ~17 nm diameter FePt nanoparticles are obtained.

To gain better control over both the stoichiometry and the internal structure of FePt nanoparticles, $Na_2Fe(CO)_4$ has been used to replace $Fe(CO)_5$ in the FePt nanoparticle synthesis.[32] $Na_2Fe(CO)_4$ acts as both a reducing agent and an Fe source. In this reaction, the anion Fe^{2-} from $Na_2Fe(CO)_4$ transfers two electrons to Pt^{2+}. The Pt^{2+} is reduced to metallic Pt while the Fe^{2-} is oxidized to metallic Fe, which then combines with Pt to form FePt. This assures the 1:1 stoichiometry of the final alloy materials. If the reaction is run in high-boiling tetracosane (boiling point: 389 °C), partially ordered fct FePt nanoparticles are separated. The room temperature coercivity of the particles reaches 1300 Oe ($1\ Oe = 10^3/4\pi\ A\ m^{-1}$).

2.2. Synthesis of FePt Nanoparticles via Co-reduction of Metal Salts

The use of a diol or polyalcohol (for example, ethylene glycol) to reduce metal salts to metal particles is referred to as the "polyol process".[33] By mixing and heating both an iron salt and a platinum salt with the polyol, high-quality FePt nanoparticles can be produced. For example, a slight modification of the decomposition/reduction condition by replacing $Fe(CO)_5$ with $Fe(acac)_2$ or $Fe(acac)_3$ has led to monodisperse 2–3 nm diameter FePt nanoparticles.[34–36] Reaction of $Fe(acac)_3$ and $Pt(acac)_2$ in ethylene glycol[37–39] or tetraethyl-

ADVANCED MATERIALS

ene glycol[40–43] generates FePt nanoparticles that show partially ordered fct structures. Alternatively, the stronger organic reducing agent hydrazine (N_2H_4) has been used to reduce metal salts and form FePt nanoparticle in water at low temperature.[44] In this synthesis, $H_2PtCl_6 \cdot H_2O$ and $FeCl_2 \cdot H_2O$, together with hydrazine and a surfactant, such as sodium dodecyl sulfate (SDS) or cetyltrimethylammonium bromide (CTAB), are mixed in water. The hydrazine reduces the metal cations at 70 °C, resulting in fcc-structured FePt nanoparticles.

As inorganic reducing agents, metal borohydrides are well known for metal salt reduction.[45–48] Specifically, a borohydride derivative, such as Super-Hydride, $LiBEt_3H$, is easily dissolved in ether, facilitating homogenous reduction of metal salts and formation of metal nanoparticles.[49–51] The reduction of $FeCl_2$ and $Pt(acac)_2$ mixtures in diphenyl ether by $LiBEt_3H$ in the presence of oleic acid, oleylamine, and 1,2-hexadecanediol at 200 °C, followed by refluxing at 263 °C, has led to ~4 nm FePt nanoparticles.[52] The initial molar ratio of the metal precursors is carried over to the final product, making control over the composition of the FePt much easier than in the decomposition/reduction and polyol reduction processes.

The strong reducing power of the borohydride also allows the reduction to proceed at room temperature in a pre-designed environment. Reverse micelles have been used as nanoreactors to make FePt nanoparticles. The micelles are formed using CTAB as a surfactant, 1-butanol as a co-surfactant, and octane as an oil phase.[53] Both a Fe salt and a Pt salt are dissolved in water within the nanoreactors. Adding sodium borohydride leads to the quick reduction of the salts and the formation of FePt nanoparticles. The FePt nanoparticles are also obtained by borohydride reduction of metal salts on a peptide template.[54] In general, using water as a solvent allows easy dissolution of various metal salts and application of a well-controlled biological template to synthesize FePt nanoparticles. However, at the present, the quality of the particles prepared under these low-temperature conditions has not been as high as those from the high-temperature solution-phase synthesis; boron contamination of the final product, a common problem accompanied with borohydride reduction of iron, cobalt, or nickel salts, could be a concern.

3. Surface Chemistry of FePt Nanoparticles

FePt nanoparticles are generally stabilized with alkyl carboxylic acid (RCOOH) and alkylamine (RNH_2). –COOH can covalently link to Fe, forming iron carboxylate (–COO–Fe). On the other hand, $–NH_2$, as an electron donor, prefers to bind to Pt via a coordination bond. Detailed IR spectroscopy studies on FePt nanoparticles coated with oleic acid and oleylamine indicate the presence of both $–NH_2$ and –COO– on the nanoparticle surfaces, as shown in Figure 7.[55] The –COO– acts either as a chelate ligand, binding to Fe via two O atoms, or as a monodentate molecule, linking to Fe via only one O atom.

The carboxylate- and amine-based surfactants around each FePt nanoparticle can be replaced by other similarly structured acids or amines, or by surfactants with a functional group that has a high affinity for Fe or Pt. Such surfactant exchange has been used to control the interparticle spacing in FePt nanoparticle assemblies by replacing long-chain oleate and oleylamine with short-chain acid and amine.[26] The carboxylate/amine can also be substituted by tetramethylammonium hydroxide (TMAOH).[56] The adsorption of TMAOH on the FePt surface provides each nanoparticle with an electrostatic double layer, making the FePt nanoparticles fully dispersible in aqueous solution at high concentrations. Ferromagnetic resonance measurements on these water-soluble FePt nanoparticles do not indicate oxidation of the FePt core,[56] proving the chemical stability of the FePt nanoparticles. Surfactant exchange has been further extended to coat the thiol-based molecules[57–59] and silica[60,61] over the FePt surface to make FePt nanoparticles water soluble.

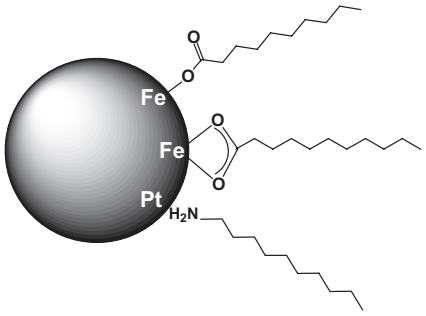

Figure 7. Schematic of binding of alkyl carboxylate and alkylamine molecules to a FePt nanoparticle.

The high affinity of FePt for S allows the preparation of multifunctional nanoparticles. FePt–CdS bimodal nanoparticles have been synthesized by coating FePt nanoparticles with amorphous CdS followed by heating, as shown in Figure 8.[62] The amorphous CdS is first deposited on the surface of FePt nanoparticles, giving core/shell structured FePt/CdS. Upon further annealing, the amorphous CdS crystallizes, and the lattice mismatch between FePt and CdS crystals makes the core/shell system metastable, leading to the formation of FePt–CdS bimodal nanoparticles. Similarly, FePt nanoparticles have been incorporated into semiconducting ZnS nanowire networks with FePt serving as the junctions.[63] The FePt nanoparticles have also been used as seeds to synthesize FePt–Ag

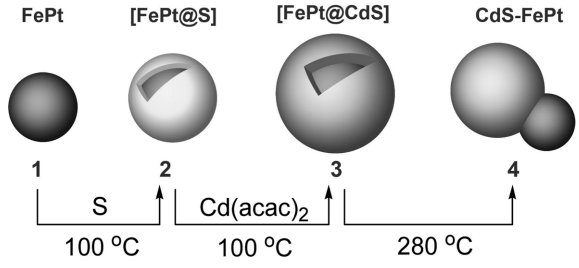

Figure 8. Schematic of a typical synthetic route to bimodal FePt–CdS nanoparticles. Reprinted with permission from [62]. Copyright 2004 American Chemical Society.

nanoparticles.[64] These bimodal nanoparticles, along with several other bimodal structures reported recently,[65–67] have two closely connected functional units, and may exhibit novel magnetic and optical properties that can be tuned by controlling the interface interactions between the two units.[68]

4. Assembly of FePt Nanoparticles

4.1. Self-Assembly

Nanoparticles with size distributions less than 5 % can form close-packed arrays on a variety of substrates as the solvent from the particle dispersion is allowed to evaporate. Such a self-assembly process into a long-range-ordered structure may be comparable with crystallization, where elements rearrange themselves into a periodic crystal structure. In a self-assembled nanoparticle superlattice, the nanoparticles act as the elements. In contrast to a crystal structure, where strong chemical bonds are usually present, nanoparticle superlattices often do not have such strong chemical interactions; instead, the particles are linked by weak hydrogen bond, van der Waals, and electric/magnetic dipole interactions.

Stabilized with oleate and oleylamine, the monodisperse FePt nanoparticles are surrounded by a layer of hydrocarbon and can serve as excellent building blocks for constructing nanoparticle superlattices through van der Waals and magnetic interactions. Colloidal crystals of monodisperse FePt nanoparticles have been grown by a three-layer technique based on slow diffusion of a non-solvent (methanol) into the bulk of a concentrated FePt nanoparticle dispersion through a buffer layer of a third component (2-propanol).[69] To control the interparticle spacing within the superlattice, surfactant exchange on the surface of the particles is performed before the self-assembly. Figure 9 shows two TEM images of the 6 nm FePt nanoparticle superlattices grown on amorphous carbon surfaces.[26] Figure 9A shows the assembly of the particles coated with oleate and oleylamine, while Figure 9B shows the particles coated with hexanoate/hexylamine. The interparticle spacing in Figure 9A is around 5 nm. That is twice as wide as the distance given by the C18 chain (~2.5 nm) in the oleate and oleylamine molecules, while in Figure 9B the spacing is closer to 1 nm due to the thin-layer coating on the particles.

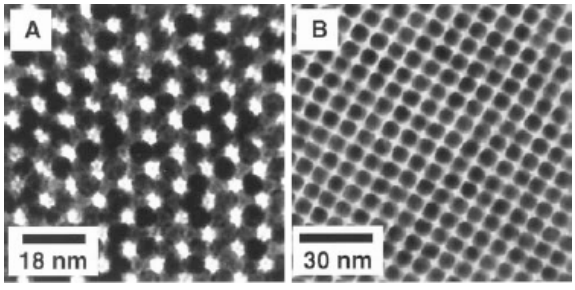

Figure 9. TEM images of A) the oleate/oleylamine coated 6 nm FePt and B) the hexanoate/hexylamine coated 6 nm FePt nanoparticle superlattices. The particles in (B) are obtained by replacing oleate/oleylamine on the surface of the particles in (A) by hexanoate/hexylamine. Reprinted with permission from [26]. Copyright 2000 American Association for the Advancement of Science.

4.2. Polymer-Mediated Self-Assembly

A solid substrate can be modified with multifunctional molecules that further replace the surfactant around nanoparticles, forming a monolayer assembly of the nanoparticles on the substrate surface. This self-assembly technique is known as molecule-mediated self-assembly and is commonly used for construction of various nanocomposite films with controlled film thicknesses.[70–76] The assembly technique has been extended to produce composite assemblies of polyethylenimine (PEI)-FePt,[52,77] phospholipid-FePt,[78] and oleic acid/oleylamine-FePt.[79] Characterizations of the layered PEI-FePt structure via X-ray reflectivity and atomic force microscopy indicate that the PEI-mediated FePt assemblies have well-controlled thicknesses.[52] The FePt nanoparticles have also been assembled on a Si/SiO_2 substrate using (3-(2-aminoethylamino)propyl)trimethoxysilane as a coupling layer.[80] Polymerization of the $–Si(OCH_3)_3$ group on the SiO_2 surface yields a strong, planar, polymeric –Si–O– network, and the $–NH_2$ group is used to bind FePt nanoparticles via surfactant exchange reaction. The assembled two-dimensional array of FePt nanoparticles is extremely robust and can withstand annealing up to 800 °C without aggregation.

4.3. Patterned Self-Assembly

The combination of physical patterning tools with self-assembly has led to patterned self-assembly of FePt nanoparticles. For example, optical lithography and self-assembly have been used to form patterned FePt nanoparticle arrays.[81] A silicon wafer with a photoresist film with patterned holes made by UV lithography can be used as a template to direct the self-assembly of FePt nanoparticles. The FePt nanoparticle dispersion is dropped onto the patterned holes. After removal of the photoresist, a patterned disk of the self-assembled FePt nanoparticles with an average diameter of 2 μm and a height of 250 nm is obtained. Alternatively, a focused laser beam has been applied for direct thermal patterning of a self-assembled FePt nanoparticle array under ambient conditions.[82] The beam can locally heat a small area of the self-assembled array on an insulating substrate. The heating carbonizes the surfactant around the particles and strengthens the linkage between them. The unexposed FePt particle assembly can be washed away with fresh solvent, leaving patterned islands of FePt nanoparticles. Selective adsorption of FePt nanoparticles on a modified octadecyltrichlorosilane assembly has also been achieved. A conducting cantilever in a scanning probe microscope with a positive-biased pulse voltage is applied to the assembly, oxidizing the terminal alkane groups which are then capable of absorbing FePt nanoparticles via surfactant ex-

ADVANCED MATERIALS

change, yielding well-aligned sub-100 nm dot arrays with sub-100 nm periodicity.[83] More conveniently, the FePt nanoparticles can be patterned by a diblock copolymer template.[84]

5. Structural and Magnetic Properties of FePt Nanoparticles

As synthesized, FePt particles usually possess a chemically disordered fcc structure. Thermal annealing is needed to convert the fcc structure to the highly anisotropic fct structure and to transform the particles into room-temperature nanoscale ferromagnets. The change of the internal particle structure upon annealing depends on annealing temperature, annealing time, and Fe and Pt composition. TEM,[85] XRD,[27] and Kerr-effect measurements[86] on the annealed $Fe_{52}Pt_{48}$ particle assemblies show that the onset of this structure change occurs at about 500 °C. Detailed XRD studies on FePt nanoparticle assemblies show that, with respect to the equiatomic composition, the *c* parameter changes mostly in the Pt-rich compositions and the *a* parameter changes mostly in the Fe-rich compositions. This causes the fct structure to be maximized near the Fe/Pt 50:50 composition.[87]

The as-synthesized FePt nanoparticles are superparamagnetic at room temperature. This is consistent with the low magneto-crystalline anisotropy of the fcc-structured FePt. Their magnetic properties are composition dependent and are affected by Fe–Pt interactions within the particles.[88–90] A relatively large H_c (~4000 Oe) of the particles at 5 K may also indicate the strong surface effect of the small FePt nanoparticles.[91,92] The room-temperature coercivities of the annealed FePt nanoparticle assemblies increase with annealing time and temperature,[26,27,93] reaching a maximum value with the assembly annealed at ~650 °C. Even higher annealing temperature eventfully destroys the nanocrystalline feature of the particles, leading to the formation of multidomain aggregates and a drop in the coercivity.[93] The coercivity of the FePt nanoparticle assembly also depends on the FePt composition. The extrapolation of a Gaussian fit of the coercivity and the composition relation yields the best composition to be $Fe_{55}Pt_{45}$.[27] This is consistent with what has been observed in physically deposited FePt thin films.[94,95]

6. Annealing-Induced Particle Aggregation and its Prevention

Although thermal annealing provides FePt nanoparticles with desired magnetic properties, one serious side effect of this annealing is the deterioration of the monodispersity of the particles. Previous in-situ TEM[85] and XRD experiments[52] have clearly shown the coalescence of the FePt particles annealed at 600 °C or above. To prevent this uncontrolled agglomeration, FePt nanoparticles should be embedded in thick organic[96] or robust inorganic[29,97–100] matrices, or assembled on the surface of a robust –Si–O– network to limit the mobility of the particles at high temperature.[101] An alternative solution to the sintering problem is to dope FePt with another element to lower the structure transformation temperature. It is known that the addition of Cu to a FePt film can reduce the transformation temperature.[102] Both the experimental evidence and the first-principles band calculation indicate that Cu in CuFePt substitutes into the Fe site in the FePt alloy.[103] The difference in free energy between the ordered and disordered phases is enhanced, and the driving force in the disorder–order transformation increases. In spherical FePt particles, alloying 4 at.-% Cu into the system has reduced the ordering temperature from 500 to 400 °C.[104] The same strategy can be applied to chemically made monodisperse FePt nanoparticles. Several classes of monodisperse ternary nanoparticles of FePtCu,[105] FePtAg,[106] FePtAu,[107,108] and FePtSb[109] have been successfully synthesized by a thermal decomposition and reduction method. The fcc to fct structure transformation temperature can be decreased to as low as 300 °C.[109]

7. Potential Applications of FePt Nanoparticles

7.1. FePt Nanoparticle Arrays for Data-Storage Applications

Current magnetic disk drives are based on longitudinal recording systems where the magnetization of the recorded bit lies in the plane of the disk. These systems contain a recording head composed of separate read and write elements, and moves in close proximity to a granular recording medium (Fig. 10A). Recording media traditionally have a magnetic storage layer that consists of weakly coupled magnetic particles of CoPtCrX alloy (X = B, Ta) with an average size of ~9 nm (Fig. 10B).[3,4] These ferromagnetic nanoparticles allow writing and storing magnetic transitions at high densities, with each recording bit containing hundreds of nanoparticles.

Self-assembled ferromagnetic FePt nanoparticle arrays are prospective magnetic-media candidates. Preliminary recording experiments on a ferromagnetic $Fe_{48}Pt_{52}$ nanoparticle array with H_c at 1800 Oe are shown in Figure 11.[26] Figure 11A

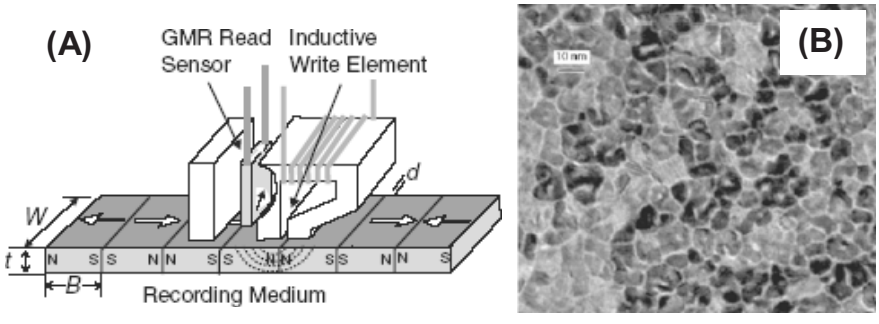

Figure 10. A) Schematic of a longitudinal recording system. B) TEM image of modern CoCrPtB recording media with an average grain diameter of 9 nm. Reprinted with permission from [4]. Copyright 2002 Institute of Physics Publishing.

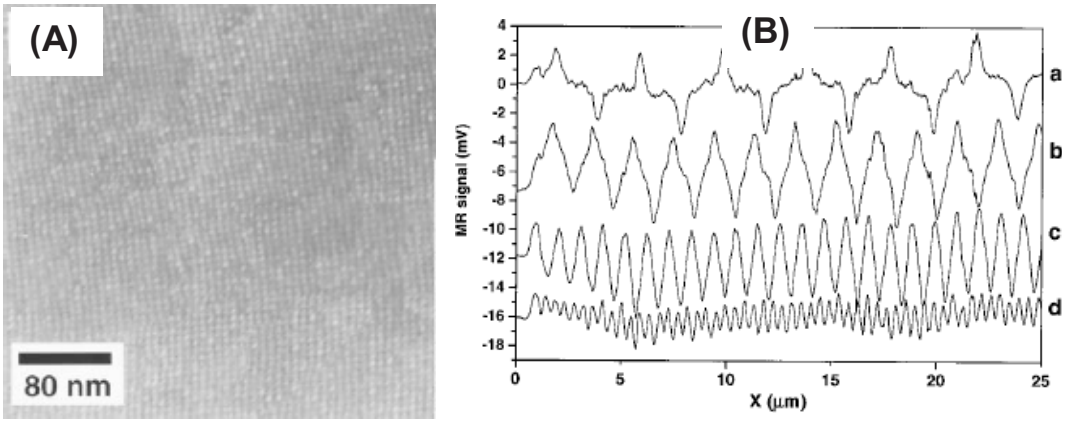

Figure 11. A) HRSEM image of a ~120 nm thick 4 nm $Fe_{48}Pt_{52}$ ferromagnetic nanoparticle assembly used for a writing experiment. B) Magneto-resistive read-back signals from the written bit transitions. The individual line scans reveal magnetization reversal transitions at linear densities of a) 500, b) 1040, c) 2140, and d) 5000 flux charges mm^{-1}. Reprinted with permission from [26]. Copyright 2000 American Association for the Advancement of Science.

is a high-resolution scanning electron microscopy (HRSEM) image of a 4 nm ferromagnetic nanoparticle assembly used for the recording demonstration. Figure 11B shows the magneto-resistive (MR) signals that are read back from the transitions by the MR sensor. The digitized read-back signals have linear densities of 500, 1000, 2000, and 5000 flux changes per millimeter, indicating that the ferromagnetic FePt nanoparticle assembly can indeed support magnetization reversal transitions.

7.2. Self-Assembled FePt-Based Nanocomposites for Permanent-Magnet Applications

Ferromagnetic FePt nanoparticles are useful building blocks for constructing permanent magnetic nanocomposites. As hard magnetic materials, FePt has a very large coercivity but a relatively low magnetic moment compared to other iron-based and magnetically soft materials, such as Fe_3Pt or Fe. A composite containing hard and soft magnets with the hard and soft phases being strongly exchange coupled could have both a large coercivity and a high magnetic moment and be capable of storing high-density magnetic energy.[110–112] To reach an optimum exchange coupling within the composite system, the soft phase should have dimensions of only around 10 nm.

Self-assembly of two different magnetic nanoparticles has been applied to produce nanocomposites with controlled nanoscale dimensions.[113] FePt and Fe_3O_4 nanoparticles can be chosen as building blocks to form binary composite assemblies that are subject to reductive annealing, converting Fe_3O_4 to Fe and transforming the fcc FePt to fct FePt. The annealing also removes the organic coating around each particle and allows interfacial diffusion between Fe and FePt, leading to nanocomposite FePt–Fe_3Pt. Figure 12 shows TEM images of the binary composite assemblies containing 4 nm Fe_3O_4 nanoparticles and 4 nm $Fe_{58}Pt_{42}$ nanoparticles (Fig. 12A) and a typical sintered nanocomposite particle (Fig. 12B) obtained from the annealing of the assembly in Figure 12A at 650 °C for 1 h. The coalesced particle is divided into two distinct phases of fct FePt and fcc Fe_3Pt, with dimensions of each phase on the order of 5 nm. The composite has an energy product (BH_{max}) value of 20.1 MGOe (1 G = 10^{-4} T), which is 37 % higher than the 14.7 MGOe obtained from the single-phase $Fe_{58}Pt_{42}$, indicating that a nanocomposite with exchange-coupled hard and soft phases does indeed have enhanced magnetic properties.

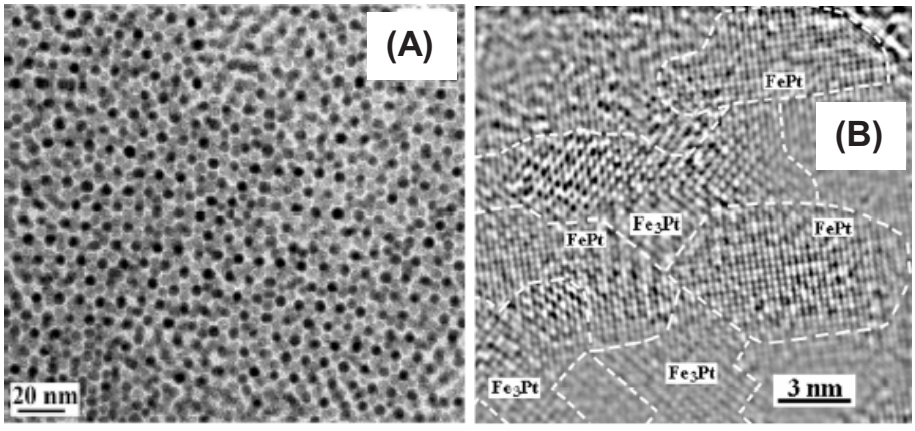

Figure 12. TEM images of binary nanoparticle assemblies of A) Fe_3O_4 (4 nm)–$Fe_{58}Pt_{42}$ (4 nm) nanoparticles and B) one sintered FePt–Fe_3Pt composite particle. Reprinted with permission from [113]. Copyright 2002 Nature Publishing Group.

ADVANCED MATERIALS

7.3. Biomedical Applications of FePt Nanoparticles

FePt nanoparticles prepared via solution-phase synthesis offer a wide range of magnetic properties and are chemically much more stable than other well-known high-moment Co and Fe nanoparticles. Their magnetic moment reaches ~1000 emu cc^{-1} (1 emu $cc^{-1} = 10^3$ A m^{-1}), comparable to Co (~1400 emu cc^{-1}) and Fe (~1700 emu cc^{-1}), and higher than commonly used iron oxide (~300–400 emu cc^{-1}). These values make the FePt nanoparticles interesting candidates for biomagnetic applications.[6]

FePt nanoparticles synthesized via the thermal decomposition/reduction method can be modified with thiol-terminated molecules via the formation of Pt–S and Fe–S bonds.[57–59,114] For example, cystamine, $S_2(CH_2CH_2NH_2)_2$, replaces oleate/oleylamine around the FePt nanoparticles to give cystamine-coated FePt nanoparticles. Similarly, vancomycin is linked to FePt nanoparticles via bis(vancomycin)cystamide. This FePt–vancomycin conjugate exhibits selective binding to Gram-negative bacteria at a concentration of 15 cfu mL^{-1} (cfu: colony forming units), which is an order of magnitude more sensitive than one of the best assays for bacteria detection based on luminescence (detection limit: 180 cfu mL^{-1}).[57,58] FePt nanoparticles have also been functionalized with mercaptoalkanoic acids and used as a general agent to bind histidine-tagged proteins,[59] forming a conjugate that is promising for instant and sensitive detection of pathogens at ultralow concentrations.

8. Concluding Remarks

Numerous studies on FePt nanoparticles and nanoparticle assemblies have revealed that the solution-phase syntheses are capable of producing high-quality FePt nanoparticles and assembling them into superlattice structures. The particles show magnetic properties ranging from superparamagnetic to ferromagnetic and are attractive as ideal models for understanding nanomagnetism. They are also promising as basic building blocks for constructing high-density data storage media and high-performance permanent magnetic nanocomposites. Their excellent chemical stability allows surfactant exchange and biomolecule attachment to be performed in various liquid media, which may lead to highly efficient and highly sensitive tools for bio-separation and bio-detection.

However, previous studies have also revealed some problems associated with these FePt nanoparticle materials, which, if not solved, will likely limit their practicality. It has been observed that a fully ordered fct-structured FePt can only be formed at high annealing temperatures at which the particles often sinter[52,115–117] or react with the substrate.[118] Magnetic studies on self-assembled FePt nanoparticle arrays show no clear evidence that a single 4 nm FePt nanoparticle is ferromagnetic at room temperature,[119] a condition that must be met for future single-particle magnetic recording. Furthermore, the magnetic direction of the FePt particles in an assembly tends to be 3D randomly orientated.[120,121]

Recent analytical and computational models predict that it is possible to obtain a chemically ordered fct structure in a FePt nanoparticle with a size larger than 3 nm,[122,123] and to align such nanoparticles in a modest magnetic field.[124] Experiments on thermally annealed silica-coated[125] and physically deposited[126] FePt nanoparticles show that single FePt nanoparticles are indeed ferromagnetic and can be partially aligned in a magnetic field,[125] unless the FePt nanoparticles are too small (smaller than 2 nm).[126] It is further demonstrated that the shape of a magnetic nanoparticle can be used to induce texture of each particle in a self-assembled nanoparticle array.[127] These indicate that the goal in fabrication of magnetically aligned FePt nanoparticle arrays is surely to be achieved in the near future and that detailed studies on nanomagnetism of these nanoparticles for advanced applications are then warranted.

Received: July 16, 2005
Published online: January 24, 2006

[1] A. H. Morrish, *The Physical Principles of Magnetism*, Wiley, New York **1965**, Ch. 7.
[2] K. M. Unruh, C. L. Chien, in *Nanomaterials: Synthesis, Properties and Applications* (Eds: A. S. Edelstein, R. C. Cammarata), Institute of Physics Publishing, Bristol, UK **1996**, Ch. 14.
[3] D. Weller, M. E. Doerner, *Annu. Rev. Mater. Sci.* **2000**, *30*, 611.
[4] A. Moser, K. Takano, D. T. Margulies, M. Albrecht, Y. Sonobe, Y. Ikeda, S. Sun, E. E. Fullerton, *J. Phys. D: Appl. Phys.* **2002**, *35*, R157.
[5] A. Jordan, R. Scholz, P. Wust, H. Fähling, R. Felix, *J. Magn. Magn. Mater.* **1999**, *201*, 413.
[6] Q. A. Pankhurst, J. Connolly, S. K. Jones, J. Dobson, *J. Phys. D: Appl. Phys.* **2003**, *36*, R167.
[7] T. Neuberger, B. Schöpf, H. Hofmann, M. Hofmann, B. von Rechenber, *J. Magn. Magn. Mater.* **2005**, *293*, 483.
[8] O. Gutfleisch, J. Lyubina, K.-H. Müller, L. Schultz, *Adv. Eng. Mater.* **2005**, *7*, 208.
[9] T. Burkert, O. Eriksson, S. I. Simak, A. V. Ruban, B. Sanyal, L. Nordström, J. M. Wills, *Phys. Rev. B: Condens. Matter Mater. Phys.* **2005**, *71*, 134 411.
[10] G. Brown, B. Kraczek, A. Janotti, T. C. Schulthess, G. M. Stocks, D. D. Johnson, *Phys. Rev. B: Condens. Matter Mater. Phys.* **2003**, *68*, 052 405.
[11] O. Kitakami, S. Okamoto, N. Kikuchi, Y. Shimada, *Jpn. J. Appl. Phys., Part 2* **2003**, *42*, 455.
[12] J. B. Staunton, S. Ostanin, S. S. A. Razee, B. L. Gyorffy, L. Szunyogh, B. Ginatempo, E. Bruno, *Phys. Rev. Lett.* **2004**, *93*, 257 204.
[13] K. R. Coffey, M. A. Parker, J. K. Howard, *IEEE Trans. Magn.* **1995**, *31*, 2737.
[14] N. Li, B. M. Lairson, *IEEE Trans. Magn.* **1999**, *35*, 1077.
[15] R. A. Ristau, K. Barmak, L. H. Lewis, K. R. Coffey, J. K. Howard, *J. Appl. Phys.* **1999**, *86*, 4527.
[16] C. P. Luo, S. H. Liou, D. J. Sellmyer, *J. Appl. Phys.* **2000**, *87*, 6941.
[17] B. Bian, D. E. Laughlin, K. Sato, Y. Hirotsu, *J. Appl. Phys.* **2000**, *87*, 6962.
[18] C. P. Luo, S. H. Liou, L. Gao, Y. Liu, D. J. Sellmyer, *Appl. Phys. Lett.* **2000**, *77*, 2225.
[19] C.-M. Kuo, P. C. Kuo, *J. Appl. Phys.* **2000**, *87*, 419.
[20] S. Stappert, B. Rellinghaus, M. Acet, E. F. Wassermann, *J. Cryst. Growth* **2003**, *252*, 440.
[21] M. Green, *Chem. Commun.* **2005**, 3002.
[22] M. A. Willard, L. K. Kurihara, E. E. Carpenter, S. Calvin, V. G. Harris, *Int. Mater. Rev.* **2004**, *49*, 125.
[23] B. L. Cushing, V. L. Kolesnichenko, C. J. O'Connor, *Chem. Rev.* **2004**, *104*, 3893.

[24] J. Park, E. Lee, N.-M. Hwang, M. Kang, S. C. Kim, Y. Hwang, J.-G. Park, H.-J. Noh, J.-Y. Kim, J.-H. Park, T. Hyeon, *Angew. Chem. Int. Ed.* **2005**, *44*, 2872.
[25] D. L. Huber, *Small* **2005**, *1*, 482.
[26] S. Sun, C. B. Murray, D. Weller, L. Folks, A. Moser, *Science* **2000**, *287*, 1989.
[27] S. Sun, E. E. Fullerton, D. Weller, C. B. Murray, *IEEE Trans. Magn.* **2001**, *37*, 1239.
[28] S. Momose, H. Kodama, T. Uzumaki, A. Tanaka, *Jpn. J. Appl. Phys., Part 1* **2005**, *44*, 1147.
[29] M. Chen, J. P. Liu, S. Sun, *J. Am. Chem. Soc.* **2004**, *126*, 8394.
[30] X. Teng, H. Yang, *J. Am. Chem. Soc.* **2003**, *125*, 14 559.
[31] X. Teng, D. Black, N. J. Watkins, Y. Gao, H. Yang, *Nano Lett.* **2003**, *3*, 261.
[32] L. E. M. Howard, H. L. Nguyen, S. R. Giblin, B. K. Tanner, I. Terry, A. K. Hughes, J. S. O. Evans, *J. Am. Chem. Soc.* **2005**, *127*, 10 140.
[33] F. Fiévet, J. P. Lagier, M. Figlarz, *MRS Bull.* **1989**, *14*, 29.
[34] K. E. Elkins, T. S. Vedantam, J. P. Liu, H. Zeng, S. Sun, Z. L. Wang, Y. Ding, *Nano Lett.* **2003**, *3*, 1647.
[35] M. Nakaya, Y. Tsuchiya, K. Ito, Y. Oumi, T. Sano, T. Teranishi, *Chem. Lett.* **2004**, 130.
[36] C. Liu, X. Wu, T. Klemmer, N. Shukla, X. Yang, D. Weller, A. G. Roy, M. Tanase, D. Laughlin, *J. Phys. Chem. B* **2004**, *108*, 6121.
[37] B. Jeyadevan, A. Hobo, K. Urakawa, C. N. Chinnasamy, K. Shinoda, K. Tohji, *J. Appl. Phys.* **2003**, *93*, 7574.
[38] T. Iwaki, Y. Kakihara, T. Toda, M. Abdullah, K. Okuyama, *J. Appl. Phys.* **2003**, *94*, 6807.
[39] R. Harpeness, A. Gedanken, *J. Mater. Chem.* **2005**, *15*, 698.
[40] B. Jeyadevan, K. Urakawa, A. Hobo, N. Chinnasamy, K. Shinoda, K. Tohji, D. D. J. Djayaprawira, M. Tsunoda, M. Takahashi, *Jpn. J. Appl. Phys., Part 2* **2003**, *42*, 350.
[41] K. Sato, B. Jeyadevan, K. Tohji, *J. Magn. Magn. Mater.* **2005**, *289*, 1.
[42] R. Minami, Y. Kitamoto, T. Chikata, S. Kato, *Electrochim. Acta* **2005**, *51*, 864.
[43] Y. Kitamoto, R. Minami, Y. Shibata, T. Chikata, S. Kato, *IEEE. Trans. Magn.* **2005**, *41*, 3880.
[44] P. Gibot, E. Tronc, C. Chanéac, J. P. Lolivet, D. Fiorani, A. M. Testa, *J. Magn. Magn. Mater.* **2005**, *290–291*, 555.
[45] H. I. Schlesinger, H. C. Brown, A. E. Finholt, J. R. Gilbreath, H. R. Hockstrue, E. K. Hyde, *J. Am. Chem. Soc.* **1953**, *75*, 215.
[46] L. Yiping, G. C. Hadjipanayis, C. M. Sorensen, K. J. Klabunde, *J. Magn. Magn. Mater.* **1989**, *79*, 321.
[47] G. N. Glavee, K. J. Klabunde, C. M. Sorensen, G. C. Hadjipanayis, *Langmuir* **1994**, *10*, 4726.
[48] Y.-P. Sun, H. W. Rollins, R. Guduru, *Chem. Mater.* **1999**, *11*, 7.
[49] H. Bonnemann, W. Brijoux, T. Joussen, *Angew. Chem. Int. Ed. Engl.* **1990**, *29*, 273.
[50] H. Bonnemann, R. Brinkmann, R. Koppler, P. Neiteler, J. Richter, *Adv. Mater.* **1992**, *4*, 804.
[51] S. Sun, C. B. Murray, *J. Appl. Phys.* **1999**, *85*, 4325.
[52] S. Sun, S. Anders, T. Thomson, J. E. E. Baglin, M. F. Toney, H. F. Hamann, C. B. Murray, B. D. Terris, *J. Phys. Chem. B* **2003**, *107*, 5419.
[53] E. E. J. A. Sims, J. A. Wienmann, W. L. Zhou, C. J. O'Connor, *J. Appl. Phys.* **2000**, *87*, 5615.
[54] B. D. Reiss, C. Mao, D. J. Solis, K. S. Ryan, T. Thomson, A. M. Belcher, *Nano Lett.* **2004**, *4*, 1127.
[55] N. Shukla, C. Liu, P. M. Jones, D. Weller, *J. Magn. Magn. Mater.* **2003**, *266*, 178.
[56] V. Salgueiriño-Maceira, L. M. Liz-Marzán, M. Farle, *Langmuir* **2004**, *20*, 6946.
[57] H. Gu, P.-L. Ho, K. W. T. Tsang, C.-W. Yu, B. Xu, *Chem. Commun.* **2003**, 1966.
[58] H. Gu, P.-L. Ho, K. W. T. Tsang, L. Wang, B. Xu, *J. Am. Chem. Soc.* **2003**, *125*, 15 702.
[59] C. Xu, K. Xu, H. Gu, X. Zhong, Z. Guo, R. Zheng, X. Zhang, B. Xu, *J. Am. Chem. Soc.* **2004**, *126*, 3392.
[60] M. Aslam, L. Fu, S. Li, V. P. Dravid, *J. Colloid Interface Sci.* **2005**, *290*, 444.
[61] V. Salgueiriño-Maceira, M. A. Correa-Duarte, M. Farle, *Small* **2005**, *1*, 1073.
[62] H. Gu, R. Zheng, X. Zhang, B. Xu, *J. Am. Chem. Soc.* **2004**, *126*, 5664.
[63] H. Gu, R. Zheng, H. Liu, X. Zhang, B. Xu, *Small* **2005**, *1*, 402.
[64] H. Gu, Z. Yang, J. Gao, C. K. Chang, B. Xu, *J. Am. Chem. Soc.* **2005**, *127*, 34.
[65] T. Mokari, E. Rothenberg, I. Popov, R. Costi, U. Banin, *Science* **2004**, *304*, 1787.
[66] T. Teranishi, Y. Inoue, M. Nakaya, Y. Oumi, T. Sano, *J. Am. Chem. Soc.* **2004**, *126*, 9914.
[67] H. Yu, M. Chen, P. M. Rice, S. X. Wang, R. L. White, S. Sun, *Nano Lett.* **2005**, *5*, 379.
[68] Y. Li, Q. Zhang, A. N. Nurmikko, S. Sun, *Nano Lett.* **2005**, *5*, 1689.
[69] E. Shevchenko, D. Talapin, A. Kornowski, F. Wiekhorst, J. Kotzler, M. Haase, A. Rogach, H. Weller, *Adv. Mater.* **2002**, *14*, 287.
[70] G. Decher, *Science* **1997**, *277*, 1232.
[71] Y. Liu, A. Wang, R. Claus, *J. Phys. Chem. B* **1997**, *101*, 1385.
[72] T. Cassagneau, T. E. Mallouk, J. H. Fendler, *J. Am. Chem. Soc.* **1998**, *120*, 7848.
[73] J. Schmitt, P. Machtle, D. Eck, H. Mohwald, C. A. Helm, *Langmuir* **1999**, *15*, 3256.
[74] N. A. Kotov, *MRS Bull.* **2001**, *26*, 992.
[75] J. F. Hicks, Y. Seok-Shon, R. W. Murray, *Langmuir* **2002**, *18*, 2288.
[76] F. Hua, T. Cui, Y. Lvov, *Langmuir* **2002**, *18*, 6712.
[77] S. Sun, S. Anders, H. Hamann, J.-U. Thiele, J. E. E. Baglin, T. Thomson, E. E. Fullerton, C. B. Murray, B. D. Terris, *J. Am. Chem. Soc.* **2002**, *124*, 2884.
[78] A. Terheiden, B. Rellinghaus, S. Stappert, M. Acet, C. Mayer, *J. Chem. Phys.* **2004**, *121*, 510.
[79] M. Acet, C. Mayer, O. Muth, A. Terheiden, G. Dyker, *J. Cryst. Growth* **2005**, *285*, 365.
[80] A. C. C. Yu, M. Mizuno, Y. Sasaki, M. Inoue, H. Kondo, I. Ohta, D. Djayaprawira, M. Takahashi, *Appl. Phys. Lett.* **2003**, *82*, 4352.
[81] M. Chen, D. E. Nikles, H. Yin, S. Wang, J. W. Harrell, S. A. Majetich, *J. Magn. Magn. Mater.* **2003**, *266*, 8.
[82] H. F. Hamann, S. I. Woods, S. Sun, *Nano Lett.* **2003**, *3*, 1643.
[83] Y. Sasaki, M. Mizuno, A. C. C. Yu, T. Miyauchi, D. Hasegawa, T. Ogawa, M. Takahashi, B. Jeyadevan, K. Tohji, K. Sato, S. Hisano, *IEEE Trans. Magn.* **2005**, *41*, 660.
[84] S. Darling, N. A. Yufa, A. L. Cisse, S. D. Bader, S. J. Sibener, *Adv. Mater.* **2005**, *17*, 2446.
[85] Z. R. Dai, S. Sun, Z. L. Wang, *Nano Lett.* **2001**, *1*, 443.
[86] D. Weller, S. Sun, C. B. Murray, L. Folks, A. Moser, *IEEE Trans. Magn.* **2001**, *37*, 2185.
[87] T. J. Klemmer, N. Shukla, C. Liu, X. W. Wu, E. B. Svedberg, O. Mryasov, R. W. Chantrell, D. Weller, M. Tanase, D. E. Laughlin, *Appl. Phys. Lett.* **2002**, *81*, 2220.
[88] M. Ulmeanu, C. Antoniak, U. Wiedwald, M. Farle, S. Sun, *Phys. Rev. B: Condens. Matter Mater. Phys.* **2004**, *69*, 054 417.
[89] H.-G. Boyen, K. Fauth, B. Stahl, P. Ziemann, G. Kastle, F. Weigl, F. Banhart, M. Hessler, G. Schutz, N. S. Gajbhiye, J. Ellrich, H. Hahn, M. Buttner, M. G. Garnier, P. Oelhafen, *Adv. Mater.* **2005**, *17*, 574.
[90] O. Robach, C. Quiros, S. M. Valvidares, C. J. Walker, S. Ferrer, *J. Magn. Magn. Mater.* **2003**, *264*, 202.
[91] B. Stahl, N. S. Gajbhiye, G. Wilde, D. Kramer, J. Ellrich, M. Ghafari, H. Hahn, H. Gleiter, J. Weißmüller, R. Würschum, P. Schlossmacher, *Adv. Mater.* **2002**, *14*, 24.
[92] B. Stahl, J. Ellrich, R. Theissmann, M. Ghafari, S. Bhattacharya, H. Hahn, N. S. Gajbhiye, D. Kramer, R. N. Viswanath, J. Weissmüller, H. Gleiter, *Phys. Rev. B: Condens. Matter Mater. Phys.* **2003**, *67*, 014 422.
[93] H. Zeng, S. Sun, T. S. Vedantam, J. P. Liu, Z. R. Dai, Z. L. Wang, *Appl. Phys. Lett.* **2002**, *80*, 2583.

[94] M. Watanabe, M. Homma, *Jpn. J. Appl. Phys., Part 1* **1996**, *35*, 1264.
[95] D. Weller, A. Moser, L. Folks, M. E. Best, L. Wen, M. F. Toney, M. Schwickert, J.-U. Thiele, M. F. Doerner, *IEEE Trans. Magn.* **2000**, *36*, 10.
[96] S. Momose, H. Koroyoshi, N. Ihara, T. Uzumaki, A. Tanaka, *Jpn. J. Appl. Phys., Part 2* **2003**, *42*, 1252.
[97] H. Zeng, J. Li, Z. L. Wang, J. P. Liu, S. Sun, *Nano Lett.* **2004**, *4*, 187.
[98] C. Liu, X. Wu, T. Klemmer, N. Shukla, D. Weller, *Chem. Mater.* **2005**, *17*, 620.
[99] K. Elkins, D. Li, N. Poudyal, V. Nandwana, Z. Jin, K. Chen, J. P. Liu, *J. Phys. D: Appl. Phys.* **2005**, *38*, 2306.
[100] M.-P. Chen, K. Kuroishi, Y. Kitamoto, *IEEE Trans. Magn.* **2005**, *41*, 3376.
[101] M. Mizuno, Y. Sasaki, A. C. C. Yu, M. Inoue, *Langmuir* **2004**, *20*, 11 305.
[102] T. Maeda, T. Kai, A. Kikitsu, T. Nagase, J.-I. Akiyama, *Appl. Phys. Lett.* **2002**, *80*, 2147.
[103] T. Kai, T. Maeda, A. Kikitsu, J. Akiyama, T. Nagase, T. Kishi, *J. Appl. Phys.* **2004**, *95*, 609.
[104] Y. K. Takahashi, M. Ohnuma, K. Hono, *J. Magn. Magn. Mater.* **2002**, *246*, 258.
[105] X. C. Sun, S. S. Kang, J. W. Harrell, D. E. Nikles, *J. Appl. Phys.* **2003**, *93*, 7337.
[106] S. S. Kang, D. E. Nikles, J. W. Harrell, *J. Appl. Phys.* **2003**, *93*, 7178.
[107] S. S. Kang, Z. Y. Jia, D. E. Nikles, J. W. Harrell, *IEEE Trans. Magn.* **2003**, *39*, 2753.
[108] Z. Jia, S. Kang, D. E. Nikles, J. W. Harrel, *IEEE Trans. Magn.* **2005**, *41*, 3385.
[109] Q. Yan, T. Kim, A. Purkayastha, P. G. Ganesan, M. Shima, G. Ramanath, *Adv. Mater.* **2005**, *17*, 2233.
[110] E. F. Kneller, R. Hawig, *IEEE Trans. Magn.* **1991**, *27*, 3588.
[111] R. Skomski, J. M. D. Coey, *Phys. Rev. B: Condens. Matter Mater. Phys.* **1993**, *48*, 15 812.
[112] T. Schrefl, H. Kronmuller, J. Fidler, *J. Magn. Magn. Mater.* **1993**, *127*, L273.
[113] H. Zeng, J. Li, J. P. Liu, Z. L. Wang, S. Sun, *Nature* **2002**, *420*, 395.
[114] R. Hong, N. O. Fischer, T. Emrick, V. M. Rotello, *Chem. Mater.* **2005**, *17*, 4617.
[115] S. Anders, M. F. Toney, T. Thomson, R. F. Farrow, J.-U. Thiele, B. D. Terris, S. Sun, C. B. Murray, *J. Appl. Phys.* **2003**, *93*, 6299.
[116] S. Anders, M. F. Toney, T. Thomson, J.-U. Thiele, B. D. Terris, S. Sun, C. B. Murray, *J. Appl. Phys.* **2003**, *93*, 7343.
[117] T. Thomson, M. F. Toney, S. Raoux, S. L. Lee, S. Sun, C. B. Murray, B. D. Terris, *J. Appl. Phys.* **2004**, *96*, 1197.
[118] T. Thomson, M. F. Toney, S. Raoux, J. E. E. Baglin, S. L. Lee, S. Sun, B. D. Terris, *J. Appl. Phys.* **2004**, *95*, 6738.
[119] G. A. Held, H. Zeng, S. Sun, *J. Appl. Phys.* **2004**, *95*, 1481.
[120] S. Kang, Z. Jia, S. Shi, D. E. Nikles, J. W. Harrel, *Appl. Phys. Lett.* **2005**, *86*, 62 503.
[121] H. Kodama, S. Momose, T. Sugimoto, T. Uzumaki, A. Tanaka, *IEEE Trans. Magn.* **2005**, *41*, 665.
[122] M. Muller, K. Albe, *Phys. Rev. B: Condens. Matter Mater. Phys.* **2005**, *72*, 094 203.
[123] R. V. Chepulskii, W. H. Butler, *Phys. Rev. B: Condens. Matter Mater. Phys.* **2005**, *72*, 134 205.
[124] J. W. Harrel, S. Kang, Z. Jia, D. E. Nikles, *Appl. Phys. Lett.* **2005**, *87*, 202 508.
[125] S. Yamamoto, Y. Morimoto, T. Ono, M. Takano, *Appl. Phys. Lett.* **2005**, *87*, 32 503.
[126] T. Miyazaki, O. Kitakami, S. Okamoto, Y. Shimada, Z. Akase, Y. Murakami, D. Shindo, Y. K. Takahashi, K. Hono, *Phys. Rev. B: Condens. Matter Mater. Phys.* **2005**, *72*, 144 419.
[127] H. Zeng, P. M. Rice, S. X. Wang, S. Sun, *J. Am. Chem. Soc.* **2004**, *126*, 11 458.